

Hybrid Renewable Energy System Proposal: Offshore Wind and PV Farm with Optimally Designed LCL Filter in Datça, Aegean Sea, Turkey

Alp Karadeniz^{1*} 

¹Balıkesir University, Electrical & Electronics Engineering Department, Balıkesir, Türkiye

* akaradeniz@balikesir.edu.tr

* Orcid No: 0000-0002-0899-6581

Received: 24 September 2024

Accepted: 17 December 2024

DOI: 10.18466/cbayarfbe.1555073

Abstract

Different kinds of power electronics-based converters and inverters are used in the grid integration of Renewable Energy Systems. These power electronic based interfaces cause harmonic distortion in voltage and current of the grid. This research aims to propose and design a hybrid renewable energy system that uses Type 4 Permanent Magnet Synchronous Generator (PMSG) and Photovoltaic (PV) power generation farm for the Datça region in Turkey. Also, the study examines the optimal passive filter designs and harmonic analysis for designed hybrid renewable power system. In detail, the system has a 2 MW PV farm is designed to be combined with a 2 MW offshore wind farm (OWF) which is connected to the 120 kV common grid by a 25 kV distribution feeder. Additionally, utilizing meteorological data that is taken from Datça, Aegean Sea region, Turkey, such as wind speed and solar irradiation, as input parameters of the hybrid power generation system. After that, to study harmonic analysis and optimal filter designs, a mathematical strategy is proposed. First of all, the arithmetic mean (AM) of daily data (DD) is considered as the input value of OWF and PV system. With using these values, an optimal LCL filter design is found by a recently proposed meta-heuristic algorithm, Mountain Gazelle Optimization (MGO), algorithm. According to IEEE 519 standards, the optimization method seeks to minimize both the voltage levels in p.u. and the total harmonic distortion (THD) of current and voltage values. Moreover, the hybrid renewable power model is simulated with optimal LCL filters by using DD wind speed and solar irradiation values. Moreover, the performance analysis based on the results of AM data and DD values is studied.

Keywords: Offshore Wind Farms, Type 4 PMSG, Optimization, Harmonic, Power Quality, Photovoltaic Power Generation Farm, LCL Filter, Hybrid Power Systems.

1. Introduction

Amid the global shift towards achieving carbon neutrality in light of climate change concerns, there is a growing emphasis on renewable energy sources, particularly offshore wind power. Oil corporations are redirecting investments towards sustainable energy initiatives, while policymakers are increasingly endorsing emerging technologies. Offshore wind energy, known for its abundant and consistent nature, is leading this transition due to its expanding capacity and reduced visual impact compared to land-based wind farms. The rise of floating wind turbines is further enhancing the competitiveness of offshore wind energy, leading to a rapid proliferation of both the number and scale of offshore wind farms [1–3].

Guaranteeing consistent voltage and frequency, minimal disruptions, and low harmonic emissions are essential for upholding reliability, stability, and customer satisfaction within the power grid [4,5]. Nevertheless, as wind power plants (WPPs) integrate into the primary grid, harmonic distortion emerges as a significant issue concerning power quality [6].

Moreover, solar power is increasingly becoming a notable contributor to renewable energy in Turkey, owing to its abundant solar energy potential. Over the last decade, substantial investments have been made in photovoltaic solar plants, resulting in a deployed capacity of 6.2 GW as of June 2020, with continued growth anticipated [7]. Also, aside from the many positive effects of the hybrid renewable systems, various power electronics-based converters and inverters used for integrating OWF and Photovoltaic power generation systems into the grid can introduce harmonics into

voltage and current waveforms. These harmonics can cause issues such as transformer overheating, circuit breaker tripping, and reduced equipment lifespan, necessitating efforts to minimize them to maintain power quality standards in accordance with guidelines like IEEE 519-2014 and IEC 61000 [8].

In addition to that, in this paper, the optimal design of a series LCL filter [9], which can effectively mitigate high-frequency harmonics, is examined for systems incorporating hybrid renewable power systems, based on the arithmetic mean (AM) values of hourly data obtained from the European Commission for Datça, Muğla [10]. Moreover, AM data is used to represent the average values of wind speed and solar irradiation over a period. This is the input data used to optimize the system's harmonic filter design. Also, the decision to use average (AM) data for wind speed and solar radiation is common in system optimization studies as it simplifies the model and provides a stable basis for parameter optimization. Using average data ensures consistency and reduces the complexity introduced by extreme fluctuations in real-time data. While daily variations are acknowledged, using average values helps in developing a generalized system performance model [11]. Moreover, the decision to use the daily average wind speed and radiation values in the simulation was made to streamline the analysis and ensure consistency in results. While wind speed and radiation are indeed variable, using daily averages helps in balancing the fluctuations and provides a reasonable estimate for the system's performance over time. This methodology is common in the modelling of renewable energy systems and helps simplify complex variables for optimization purposes [12, 13]. Firstly, an objective function (OF) is formulated, encompassing the total harmonic distortion of the voltage waveform (THDV), the effective value of the voltage magnitude, and the power of the passive filter. To determine the optimal filter parameters, a recently proposed meta-heuristic optimization algorithm, the Mountain Gazelle Optimization (MGO) algorithm [14], is utilized to solve the OF. Additionally, the study investigates the impact of filter parameters on system performance in terms of power quality essentials (THD, voltage level, power factor, and power values), and provides a performance analysis for AM and DD inputs with an optimal filter.

In this paper, some important contributions are provided:

- The harmonic distortion performance of a hybrid system including Type 4 offshore wind farm accompanied with PV farm is simulated for the wind speed and solar irradiation data obtained from the European Commission for Datça, Turkey [10].
- For an objective function (OF) including the total harmonic distortion of the voltage waveform (THDV) and the system's rms voltage levels, and the harmonic distortion

constraints, the optimal design of two passive filter types, series and shunt LCL filters, is formulated.

- To find optimal parameters of the considered filter types according to the formulated problem, a meta-heuristic optimization algorithm recently proposed in the literature, Mountain gazelle optimization (MGO) algorithm, is employed. The results are obtained for the arithmetic mean (AM) of the wind speed and radiation data.
- The proposed Hybrid power system is simulated for arithmetic mean (AM) values of DD obtained from the European Commission for Datça, Turkey.
- The technique for optimal filter design with AM data is proposed in the study.
- Also, there is no study about the application of the hybrid renewable system for Datça in Turkey with power quality assessments.
- Finally, the performance analysis with respect to power quality essentials (THD, voltage level, power factor, and power values) of the filter under DD is studied.

1.1. Literature Overview

According to the literature summary, there are some studies on the employment of harmonic filters to mitigate harmonic distortion in the systems integrated with onshore, offshore wind and PV systems [9,15–23].

In one of these studies, the design and simulation of a solar photovoltaic (SPV) system integrated with the grid, employing a current-controlled voltage source converter (VSC) and LCL filter, is presented. The study aims to optimize solar power utilization, meet reactive power demand, and enhance power quality through power balance control, showcasing a 10 kW SPV array simulation with indirect current control [15].

Also, in [16], the paper studies a hybrid photovoltaic (PV)-wind-battery energy storage system connected to the utility grid via a three-phase inverter, utilizing an advanced control strategy combining fuzzy logic proportional integral derivative-improved second-order generalized integrator-quadrature signal generator-phase locked loop (FLPID-ISOGI-PLL). The proposed approach enhances power quality at consumer terminals by improving power penetration, load sharing, power factor correction, and dynamic operation while maintaining DC-AC power balance, demonstrated through MATLAB/SIMULINK simulation and hardware-in-loop (HIL) co-simulation using FPGA Virtex-7 VC-707.

In addition to that, another study [17] presents a novel approach to mitigating harmonic currents in grid-connected photovoltaic energy systems by incorporating

a phase shifting transformer into the structure of an LCL filter. This approach aims to optimize LCL filter parameters for improved harmonic mitigation, in power quality enhancement for renewable energy sources.

Moreover, in [18], the study addresses filtering issues in three-phase PV grid-connected inverters by establishing mathematical models for L and LCL filters. Simulation results demonstrate superior performance of the LCL filter over L and LC filters, with parallel resistors proving more advantageous for system stability while maintaining filtering effectiveness, confirming theoretical validity.

Additionally, in [9], the study introduces a novel approach to designing LCL filters for grid-interfaced PV systems, focusing on minimizing both filtering inefficiencies and costs. By exploring a cost-based minimization approach for filter elements, optimal designs are obtained while ensuring compliance with harmonic standards and voltage drop constraints. Simulation and experimental validation of a 10-kVA grid-connected inverter confirm the efficacy of the proposed design method, demonstrating harmonic attenuation and low total harmonic distortion.

Also, the other study [19] introduces a modular hybrid renewable energy system comprising PV array, wind turbine, battery storage, AC load, and a dump load, aimed at minimizing total project cost and maximizing reliability while minimizing unutilized surplus power. A novel iterative filter selection approach is employed to design the system, ensuring the best acceptable solution considering all design objectives. Compared to iterative-Pareto-fuzzy and particle swarm optimization techniques, this approach demonstrates superiority in total project cost while meeting load demand satisfaction.

Additionally, the paper [20] proposes a redesign of the LCL grid filter for a multimewatt medium-voltage neutral-point-clamped converter used in wind turbines, employing Selective Harmonic Elimination PWM (SHEPWM). By eliminating low-order harmonics, SHEPWM enhances efficiency compared to traditional pulse width modulation techniques like Phase Disposition PWM (PDPWM), resulting in improved converter and overall system performance, as demonstrated through experimental results.

Also, in another paper [21] analyses the impact of interleaved carriers on the harmonic performance of parallel-connected voltage source converters in wind energy systems, employing 60° clamp discontinuous pulse width modulation to minimize switching losses. It presents a systematic design procedure for line filters, incorporating an LC trap branch within the conventional LCL filter to achieve optimal filter parameter values and validates the methodology through experimental verification.

Moreover, the paper [22] proposes the integration of active filters into the control system of Type-IV wind turbines in offshore WPPs to mitigate harmonic voltage amplification. Using the extra element theorem, active filter tuning is optimized to achieve both effective harmonic reduction and adequate stability margins, demonstrated through a real-time simulation of a 270 MW offshore WPP with 3-MW wind turbines, successfully suppressing converter and grid voltage harmonics below planning levels at WPP buses.

Also, the paper [23] introduces an H robust control approach for wind turbine inverters with LCL filters, aimed at selectively filtering harmonics in offshore transmission networks amidst parameter uncertainties. By combining passive filtering with a robust high-order active filter controller, the method effectively mitigates harmonic currents injected by power converter-based turbines, outperforming traditional Proportional-Integral (PI) controllers with enhanced stability and reduced control effort across operational conditions.

Moreover, the study [24] investigates advanced techniques to improve power quality in hybrid renewable energy systems, focusing on the integration of multiple energy sources such as solar and wind. It elaborates on the role of energy storage systems, including batteries and supercapacitors, and smart grid technologies in mitigating voltage fluctuations, frequency deviations, and harmonic distortions. The results underline that effective power quality management strategies not only stabilize hybrid systems but also enhance their reliability and long-term sustainability, making them more viable for large-scale deployment. Also, the study [25] explores the optimization of harmonic mitigation strategies in hybrid energy systems by employing advanced modelling and simulation techniques. It highlights the importance of active harmonic filters and control algorithms, such as predictive and adaptive controls, in minimizing harmonic distortions caused by nonlinear loads and intermittent renewable energy sources. The paper provides a comprehensive analysis of the trade-offs between cost, performance, and energy efficiency, offering practical insights into designing robust hybrid systems for enhanced power quality. Lastly, the paper [26] provides an in-depth analysis of hybrid filters and their role in addressing power quality issues in renewable energy systems, such as harmonic distortion, reactive power imbalances, and voltage stability. It emphasizes the synergy between active and passive filtering techniques, demonstrating their combined effectiveness in improving the overall stability and efficiency of energy networks. The study also discusses the critical factors influencing filter performance, including system configuration, load characteristics, and real-time control capabilities, offering guidelines for implementing hybrid filters in practical energy distribution systems.

To compare the recently published studies, the study [24] focuses on power quality enhancement but primarily uses optimized controllers for mitigating harmonics in grid-connected hybrid systems involving either wind or solar power. Unlike this study, which combines offshore wind and PV systems, it lacks the dual-source integration.

Also, the study [25] emphasizes optimizing harmonic mitigation in hybrid wind-PV systems but does not incorporate the novel Mountain Gazelle Optimization (MGO) algorithm. Instead, traditional methods are used, making the optimization approach in this study more advanced.

Moreover, the referenced study [26] improves power quality in PV systems using hybrid filters, but it does not focus on offshore wind energy or consider the specific regional conditions of Datça, Turkey, which is a key focus of this study.

2. Modelling of The Studied System

In this section, the modelling of the studied system with the OWF and PV system is introduced.

2.1 Modelling of Hybrid Power System

The schematic of the studied system containing offshore wind farm with Type 4 PMSG turbine and PV power generation system is given in Fig. 1. It has a 120 kV 60 Hz grid system, a 47 MVA, 120/25 kV, Y/Δ transformer, a 25kV/575V, 2.5 MVA, Δ/Y transformer, and a submarine cable with 36 km length. There is an LCL filter connected to 575 V bus, which is to be optimized for improvement of the bus voltage harmonic distortion and rms levels.

In addition, the resistances and inductances of primary winding of the second one is 0.000833 p.u. and 0.025 p.u., those parameters of secondary winding seen from primary side are 8.33e-4 p.u and 0.08 p.u., and its magnetization inductance is 500 p.u. Additionally, in the system, the π model parameters of the submarine cable (Fig. 2), which is utilized for the test offshore wind farm, are taken from ABB data sheets [27, 28]. They are given in Table 1.

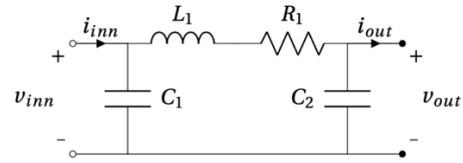


Figure 2: The equivalent π circuit model of the cable.

Table 1: The circuit parameters per km of the cable model taken from ABB data sheet.

Cable	R (mΩ/ km)	L (mH/ km)	C (μF/ km)
500 mm ² Cu cable	33.6	0.41	0.24
	$R_0(\Omega/km)$	$L_0(mH/km)$	$C_0(nF/km)$
	1000	4.1264	7.7519

To accurately model the cable in the simulations, it should be represented as series connected multiple sections considering the π model depicted in Figure 2. The required number of π -sections should be determined regarding the considered highest harmonic order and length of cable [2]. Accordingly, the submarine cable is segmented into three identical π -sections.

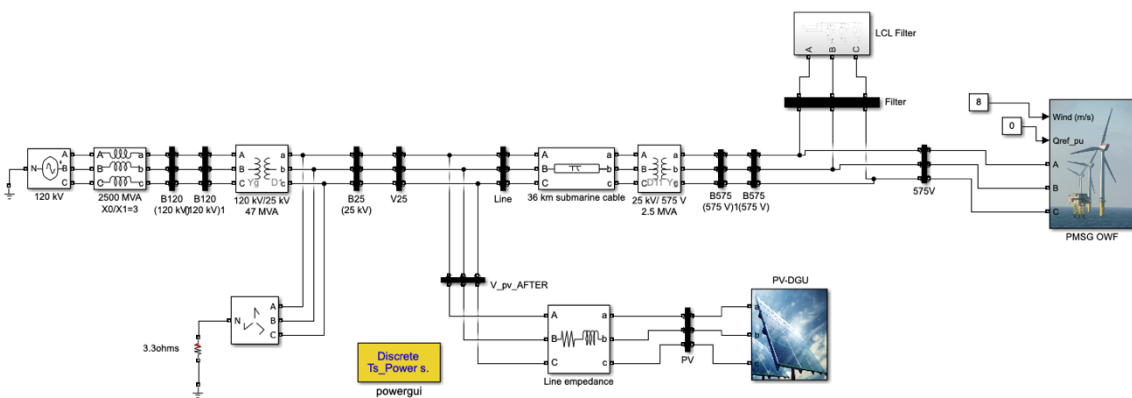


Figure 1: The studied hybrid system Simulink model.

2.2- Modelling of Wind Energy Generation System (PMSG)

In the examined system, a 2 MW wind farm is connected to a 25kV distribution network transferring power to a

120kV grid. In the farm, each turbine has a permanent synchronous generator (PMSG) and a full-scale power converter [2]. The detailed schematic of the Wind Turbine, depicted in Fig. 3, provides further insight.

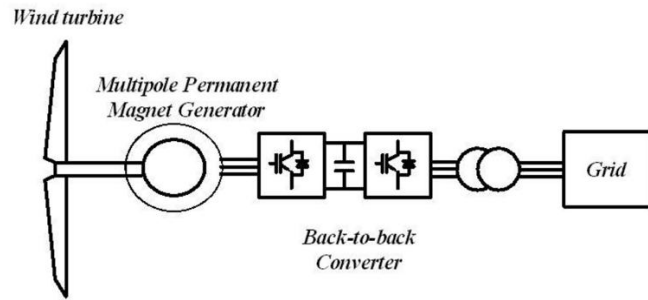


Figure 3: The schematic representation of a PMSG.

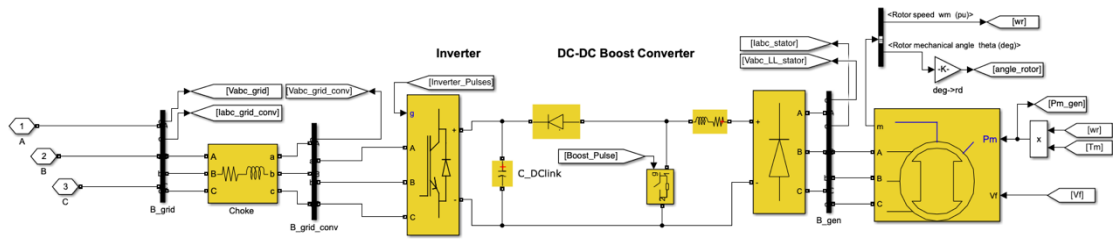


Figure 4: Under mask illustration of PMSG wind turbine block.

For the simulations, the wind speed remains constant at 15 m/s. The control system employs a torque controller to maintain speed at 1.2 per unit (pu), while the reactive power output from the wind turbine is regulated at 0 Mvar. Although the turbine output power is 1 pu of its

rated power at a wind speed of 15 m/s, for demonstration purposes of DD values throughout the optimization process, the AM value (8.85 m/s) wind speed is considered.

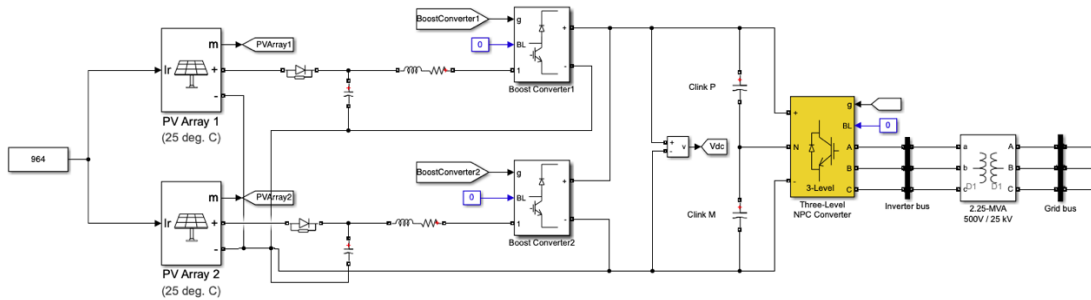


Figure 5: Under mask illustration of PV solar system block.

In the combined modelled framework, a 2 MW PV power system is considered (See Fig. 5). Furthermore, the PV system comprises two PV arrays: PV Array 1 and PV Array 2, capable of generating 1.5 MW and 500 kW, respectively, under 1000 W/m² solar irradiance and 25 degrees Celsius cell temperature. Each PV array is connected to a boost converter, with each boost being independently regulated by Maximum Power Point Trackers (MPPT) employing the Perturb and Observe method to optimize power extraction by adjusting voltage levels across the PV array terminals. The outputs from the boost converters are connected to a shared 1000

V DC bus. A three-level Neutral Point Clamped (NPC) converter transforms the 1000 V DC to approximately 500 V AC. Control of the NPC converter is managed by a DC voltage regulator tasked with maintaining the DC link voltage at 1000V. Additionally, a 2.25-MVA 500V/25kV three-phase coupling transformer links the converter to the grid. The grid configuration encompasses standard 25-kV distribution feeders and a 120-kV equivalent transmission infrastructure.

2.4- Data preparation process

This paper performs a performance analysis of the modelled system using the Typical Meteorological Year (TMY) dataset provided by the European Commission's Joint Research Centre (JRC). The TMY dataset covers the period from March 2007 to June 2020, spanning approximately 13 years, with hourly data available [10]. The Typical Meteorological Year (TMY) dataset is widely used in energy system simulations as it provides reliable, long-term meteorological data for modelling renewable energy generation. The dataset's reliability is supported by its extensive use in studies and validated by several credible sources. Moreover, the Typical Meteorological Year (TMY) dataset is widely used in renewable energy modelling for providing a representative set of climatic data over a year. It is particularly useful for simulations in regions like Datça, where long-term data is crucial for accurate forecasting. The reliability of the TMY dataset is well-documented in several studies, which confirm its accuracy in modelling renewable energy systems [29, 30].

It includes various parameters such as wind speed, solar irradiance, among others. Additionally, sample data from Datça, Turkey, located in the Aegean Sea region, is considered. The geographical coordinates of the reference point are latitude 36.656 and longitude 27.393 for the Datça area. Fig. 6 depicts the geographical position of the reference point within the Aegean Sea region.

The Datça region is selected due to its favourable wind speed and also, solar irradiations values, making it an ideal location for offshore wind and PV farm installation in the Aegean Sea. Notably, there are currently no OWF

applications in Turkey. This study aims to simulate power quality performance of the generic hybrid renewable energy generation system including offshore wind farm and PV units under the wind speed and solar irradiation values of Datça. Furthermore, the hybrid model is simulated over a 20-second scale, representing daily values for one month in the Datça dataset for June 2020. This entails linear scaling of 744 data points over the 20-second timeframe, resulting in a time representation of 0.02688 seconds per data point. Both wind speed and solar irradiation data are utilized for the OWF and PV farm in the hybrid renewable power generation system. The nominal power values for both the OWF and PV system are set at 2 MW each, corresponding to wind speeds of 15m/s and solar irradiation values of 1000 W/m². However, to reflect real-world performance, an optimal passive filter design is developed based on the arithmetic mean values (8.85 m/s for wind speed and 964 W/m² for solar irradiance) derived from the wind speed and solar irradiation data points for June 2020.

Also, the choice to use June data was based on the typical high stability and peak values of wind speed and solar irradiation observed in this period for the Datça region. By using the arithmetic mean of this data, a balanced and reliable representation of system performance has been ensured. This approach helps simplify the analysis while maintaining the accuracy of results. Variations in wind speed are integrated with different data sets (e.g., TMY) and their respective averages over a month. This method remains practical for the scope of our study while still providing valuable insights into system performance [31]. Table 2 presents the nominal and AM data for the hybrid renewable power system. In this study, AM data is utilized to formulate optimal design and conduct performance analysis.



Figure 6: Geological locations of pivot point Datça area [10].

Table 2: Data scaling of AM data.

	Nominal Data	Real data
Wind speed	15 m/s	8.8 m/s
OWF power	2 MW	1.18 MW
Solar irradiation	1000 W/m ²	966.8 W/m ²
PV power	2 MW	1.933 MW
Expected power at distribution bus (25kV)	4 MW	3.11 MW

As seen from Table 2, the nominal and AM data of OWF power and PV system power are 1.18 MW and 1.933 MW, respectively. Also, expected power rating at 25kV (PCC) bus is 3.11 MW at nominal wind speed and solar irradiation values.

Moreover, to demonstrate the DD performance of the system after optimal filter integration, 2020–June, every day at 10 a.m. for 30 days, wind speed and solar

irradiation values are considered. The reason for this is that 744 data points are not suitable to create results figures and table representations with respect to this huge data number. The hour of 10 a.m. is used because the wind speed and solar irradiation values are perfectly stable and close to their maximum values as well. Table 3 shows the DD data of wind speed and solar irradiation values for June-2022 at 10.00 am

Table 3: DD data for June-2020.

2020-June	Solar Irradiation (w/m ²)	Wind Speed (m/s)
1	947	8.21
2	996	7.79
3	924	8.07
4	972	8.34
5	981	7.31
6	947	5.79
7	968	10.69
8	907	10.97
9	992	8.07
10	933	9.79
11	985	10.48
12	821	11.03
13	994	8.97
14	978	9.15
15	967	11.45
16	1020	9.38
17	930	8.21
18	1008	7.03
19	956	10.76
20	1004	12.55
21	1020	9.45
22	1001	9.86
23	1006	7.45
24	959	8.69
25	996	8.14
26	958	10.76
27	968	10.34
28	947	3.45
29	964	7.24
30	972	9.14

2.5- Harmonic Pollution in the Studied System without Filter

Fig. 7 and Fig. 8 show the waveforms and harmonic spectrums of the voltage and current at 575 V (grid-side bus of inverter output of OWF) and 25 kV (PCC bus) buses for the system without the passive filter, respectively. The total harmonic distortion (THD) values of the respective voltages are 23.92% and 5.58 and the THD values of the respective currents are 16.77% and 43.18%. Also, V_{pu} values are 1.12 and 1.31 p.u. Thus, one can see that the system without a filter has highly distorted voltage and currents, and their THD values are over the limits defined by the IEEE-519 standard [32] given in Table 5.

3- Formulation and solution algorithm of the optimal filter design

In this section, the series and shunt LCL filters considered for harmonic mitigation in the system. Also, the optimal design of these filters is formulated, and algorithms are introduced to solve the associated optimization problems.

3.1- Introduction of Considered Passive filter types

In this study, two LCL filter types, such as series LCL and shunt LCL filters, which have high compensation capability for high-frequency harmonics, are chosen. Regarding their equivalent circuits given in Fig. 9, they are briefly introduced below:

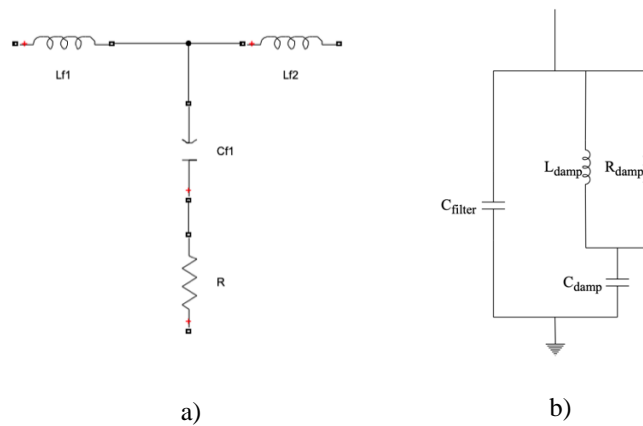


Fig 9: The single-phase representations of a) series b) shunt LCL filters.

The LCL filter configuration [9] is widely employed as an interface between converters and the utility grid due to its efficacy in smoothing converter output currents. Moreover, it demonstrates superior performance with relatively small inductor and capacitor values. The LCL filter offers enhanced attenuation of higher harmonics, enabling operation at lower switching frequencies while adhering to harmonic constraints specified in standards like IEEE-519 and IEEE-1547 [33, 34].

3.1.1- Series LCL filter

A series LCL filter consists of three main components: the inverter-side inductor, the grid-side inductor, and the filter capacitor [15]. Designing these three elements for an LCL filter typically involves solving three or more simultaneous equations, indicating the presence of multiple design objectives. But in this paper, the parameters (L_{f1} , L_{f2} , C_{f1} and R) of series LCL filter are determined by MGO algorithm. The series LCL filter is used for PV farm system and connected to primary side of the 500V/25kV bus.

3.1.2- Shunt LCL filter

The shunt LCL filter is used for OWF's output side of the inverter. A shunt LCL filter consists of four main

Table 4: The THDV (%), V_{pu} and THDI (%) values of the 575 V and 25 kV buses.

THDV(%)	
25kV Bus	23.92
575V Bus	5.58
Vpu	
25kV Bus	1.12
575V Bus	1.31
THDI(%)	
25kV Bus	16.77
575V Bus	43.18

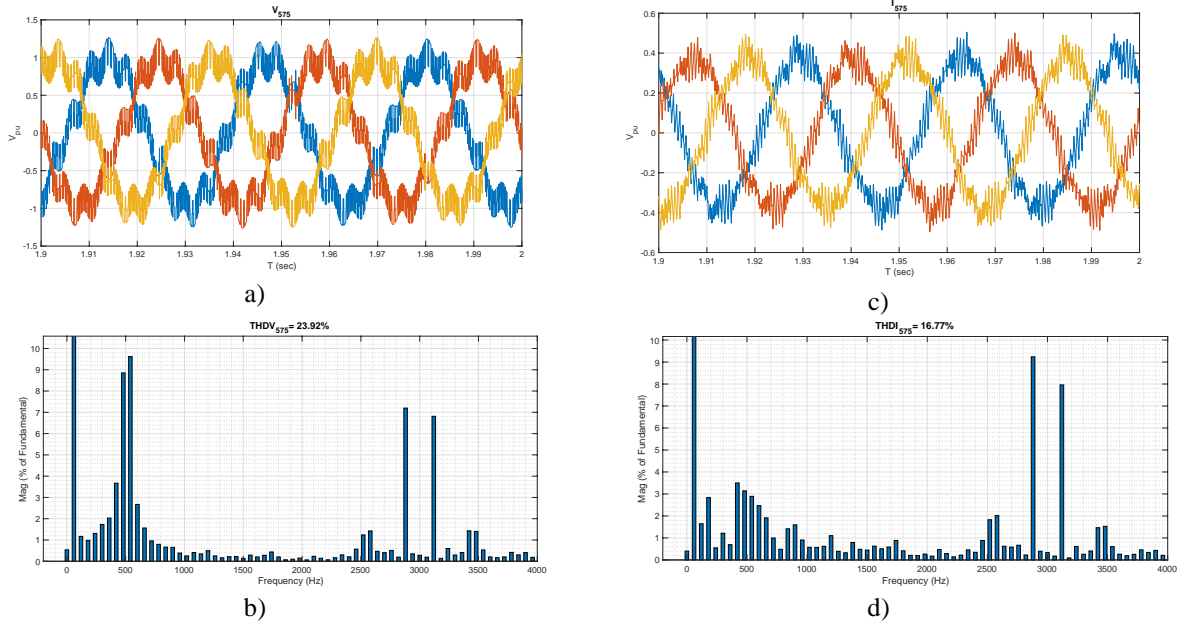


Figure 7: The (a) voltage waveforms, (b) voltage harmonic spectrums, (c) current waveforms and (d) current harmonic spectrums at the 575 V bus for the system without the filter.

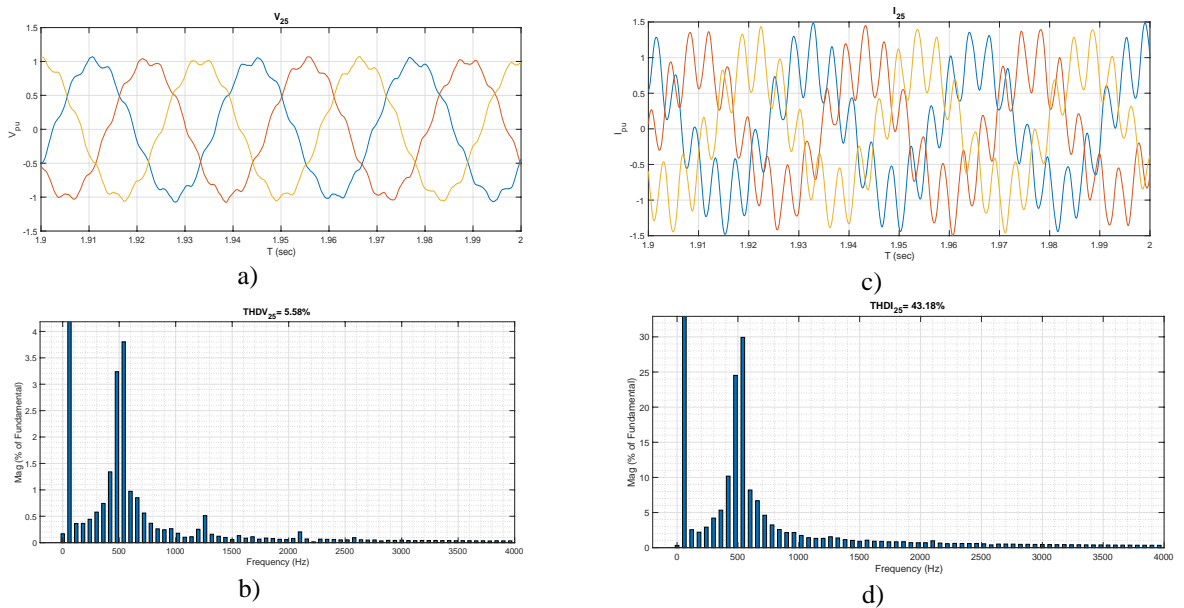


Figure 8: The (a) voltage waveforms, (b) voltage harmonic spectrums, (c) current waveforms and (d) current harmonic spectrums at the 25kV bus for the system without the filter.

Table 5: The IEEE std. 519 harmonic limits.

Bus Voltage V at PCC	Individual Harmonic (%)	Total Harmonic Distortion THD(%)
$V \leq 1.0$ kV	5.0	8.0
$1 \text{ kV} < V \leq 69$ kV	3.0	5.0
$69 \text{ kV} < V \leq 161$ kV	1.5	2.5
$161 \text{ kV} < V$	1.0	1.5

components such as; L_{damp} , C_{damp} , R_{damp} and C_{filter} . Also, designing these parameters, starting with optimally chosen f_{cutoff} value. After that, the design procedure continues with the calculation of the filter capacitance

that is shown in Eq. (1), denoted as C_{filter} , which is determined based on the cutoff frequency and the inverter inductance, represented as L_{inv} , as outlined in Eq. (5).

$$C_{filter} = \frac{1}{(2\pi \cdot f_{cutoff})^2 \cdot L_{inv}} \quad (1)$$

The damping inductance, L_{damp} , is calculated by Eq. (2).

$$L_{damp} = 5 \cdot L_{inv} \quad (2)$$

The damping capacitance, C_{damp} , can further be calculated by Eq. (3).

$$C_{damp} = \frac{C_{filter}}{2} \quad (3)$$

Then, the damping resistance, R_{damp} , can be calculated with Eq. (4).

$$R_{damp} = \sqrt{\frac{L_{damp}}{C_{damp}}} \quad (4)$$

According to [2], Eq. (5) can be utilized to determine the converter inductance. This equation is dependent on several parameters including the DC-link voltage V_{DC} , the switching frequency f_{sw} , and the peak-to-peak amplitude of the ripple current I_{rpp} . The ripple current is assumed to be 20% of the peak-to-peak nominal current.

$$L_{inv} = \frac{V_{DC}}{4 \cdot f_{sw} \cdot I_{rpp}} \quad (5)$$

In brief, f_{cutoff} is determined by optimization algorithm and L_{inv} , C_{filter} , L_{damp} , C_{damp} and R_{damp} are calculated from Eq. (1)-(5).

3.2- Problem Formulation

The parameters of series and parallel LCL passive filters are optimized to find the best suitable filter form to get less harmonically polluted operating system. In addition to that, voltage levels for all buses should be around 1 p.u. By using these passive filters, the system model is run to find optimal passive filter parameters. The objective function is created with respect to the THDV, V_{pu} and the power loss of filters values of the 25 kV bus. The 25 kV bus is selected as a candidate because it is the PCC bus which is common point of harmonic effects of OWF and PV systems. The objective function of the optimization problem can be written as follow:

Objective Function:

$$\begin{aligned} \text{minimize } F(obj) &= a * THDV_{25} + b * |V_{pu,25} - 1| + c \\ &* |sfilter_{powerloss}| + c \\ &* |pfilter_{powerloss}| \end{aligned}$$

Subject to:

$$THDV_{h-individual} \leq Max THDV_{individual}$$

$$THDI_{h-individual} \leq Max THDI_{individual}$$

$$THDV_{\%} \leq Max THDV_{\%}$$

$$THDI_{\%} \leq Max THDI_{\%}$$

a , b and c are coefficients of $THDV_{25}$ and $V_{pu,25}$. $V_{pu,25}$ is p.u. value of a phase to ground voltage value of the 25 kV bus. Also, $THDV_{25}$ value is total harmonic distortion value of the voltage at 25 kV bus. $sfilter_{powerloss}$ and $pfilter_{powerloss}$ are power values of series and parallel filters which are optimally found. $Max THDV_{individual}$ and $Max THDI_{individual}$ values are individual harmonic limits for voltage and current values restricted by IEEE 519 standarts. $THDV_{h-individual}$ and $THDI_{h-individual}$ are hth harmonic values of current and voltage. Also, $Max THDV_{\%}$ and $Max THDI_{\%}$ are determined by IEEE 519 standarts with respect to suitable voltage levels.

3.3. Solution Algorithms

To determine the optimal filter parameters, we utilize a meta-heuristic optimization algorithm called the Mountain Gazelle Optimization (MGO) algorithm [11], which has been recently proposed in the literature. The algorithms are introduced below.

3.3.1- Mountain Gazelle Optimization Algorithm (MGO)

The Mountain Gazelle Algorithm (MGO), introduced by Seyedali Mirjalili in 2022, draws inspiration from the intricate coexistence dynamics of mountain gazelles and Robinia trees in the Arabian Peninsula and nearby regions. Reflecting the territorial behaviour and migration patterns of these gazelles, MGO incorporates elements such as territorial disputes, herd formations, and extensive migrations to guide its optimization process [14].

Mathematical Model:

By mathematically, the MGO algorithm conducts optimization tasks based on four primary aspects of mountain gazelle life: herds of bachelor males, maternal herds, solitary territorial males, and migratory behaviours in search of food.

In the Mountain Gazelle Algorithm (MGO), each gazelle (X_i) can join one of three herds: maternity herds, bachelor male herds, or solitary territorial males, potentially giving birth to new gazelles within these groups. The algorithm aims to find the optimal global solution represented by an adult male gazelle within a herd's territory, with about one-third of the population expected to possess the lowest cost. Through exploitation and exploration phases facilitated by four mechanisms, MGO guides solutions towards the best outcome while exploring alternative options. Fig. 10 provides an overview of the optimization process based on the agents within MGO [14].

Territorial Solitary Males

Once male mountain gazelles reach maturity and attain sufficient strength, they establish solitary territories and exhibit pronounced territorial behaviour. Eq. (6) has been employed to formulate the model representing the territories of adult males.

$$TSM = male_{gazelle} - (r_{i_1} \times BH - r_{i_2} \times X(t)) \times F \times Cof_r \quad (6)$$

In Equation (6), the mature gazelle signifies the positional array of the optimal global solution, corresponding to the adult male gazelle. The variables r_{i_1} and r_{i_2} denote random integers, each ranging from 1 to 2. BH represents the coefficient vector for the young male herd, calculated using Eq. (7). Additionally, F is determined utilizing Eq. (8), while Cof_r denotes another coefficient vector, randomly selected and adjusted during

each iteration to enhance the exploration capability, computed with Eq. (9) [14].

$$BH = X_{ra} \times |r_1| + M_{pr} \times |r_2|, ra = \left\{ \frac{N}{3} \mid \dots N \right\} \quad (7)$$

In Eq. (7), X_{ra} represents a random solution corresponding to a young male gazelle within the interval ra . M_{pr} signifies the average number of search agents (denoted as $\frac{N}{3}$) that were randomly selected. Additionally, N represents the total number of gazelles, while r_1 and r_2 represent random values ranging between 0 and 1.

$$F = N_1(D) \times \exp \left(2 - Iter \times \left(\frac{2}{MaxIter} \right) \right) \quad (8)$$

In Eq. (8), within the dimensions of the problem, N_1 is a random number sampled from a standard distribution. The exponential function, denoted as exp , is applied. $MaxIter$ represents the total number of iterations, while $Iter$ indicates the current iteration number [14].

$$Cof_i = \begin{cases} (a + 1) + r_3, & (9) \\ a \times N_2(D), \\ r_4(D) \\ N_3(D) \times N_4(D)^2 \times \cos((r_4 \times 2) \times N_3(D)) \end{cases}$$

In Eq. (9), the parameter a is calculated using Eq. (10). Moreover, r_3 , r_4 , and $rand$ signify

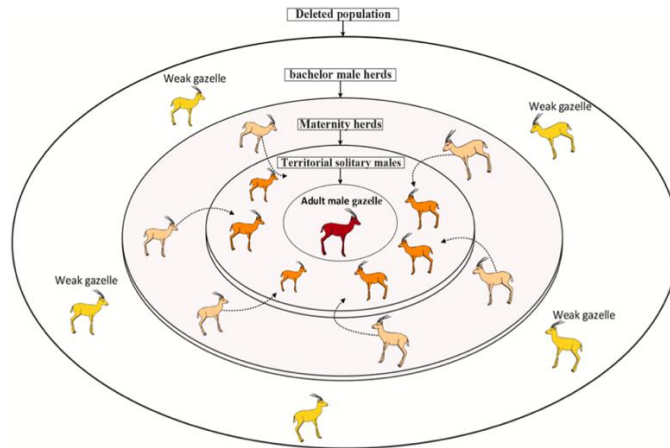


Figure 10: MGO optimization procedure [14].

three random values between 0 and 1. N_2 , N_3 , and N_4 denote random numbers drawn from a normal distribution within the problem's dimensions. Additionally, within the problem's dimensions, r_4 represents another random value between 0 and 1. Finally, cos denotes the cosine function.

$$a = -1 + Iter \times \left(\frac{-1}{MaxIter} \right) \quad (10)$$

Finally, in Eq. (10), $MaxIter$ denotes the total number of iterations, while $Iter$ represents the current iteration number [14].

Maternity Herds:

Maternity herds play a vital role in the life cycle of mountain gazelles, as these groups are responsible for birthing robust male gazelles. This behavior is mathematically formulated using Eq. (11).

$$MH = (BH + Cof_{1,r}) + (ri_3 \times male_{gazelle} - ri_4 \times X_{rand}) \times Cof_{1,r} \quad (11)$$

In Eq. (11), BH represents the vector of the impact factor of young males, which is computed using Eq. (7). $Cof_{2,r}$ and $Cof_{3,r}$ are randomly selected coefficient vectors calculated independently using Eq. (12). ri_3 and ri_4 are integer random numbers, each taking values of 1 or 2. $male_{gazelle}$ denotes the best global solution (adult male) in the current iteration. Finally, X_{rand} represents the vector position of a gazelle that is randomly selected from the entire population [14].

Bachelor Male Herds:

As male gazelles mature, they often establish territories and assert dominance over female gazelles. Eq. (12) is employed to mathematically model this behavior of gazelles.

$$BMH = (X(t) - D) + (ri_5 \times male_{gazelle} - ri_6 \times BH) \times Cof_r \quad (12)$$

In Eq. (12), $X(t)$ represents the position vector of the gazelle in the current iteration. Parameter D is computed using Eq. (13). ri_5 and ri_6 are randomly chosen integers, each taking a value of 1 or 2. $male_{gazelle}$ signifies the position vector of the male gazelle (the best solution). Additionally, BH denotes the impact factor of the young male herd, which is calculated using Eq. (7). Cof represents a randomly selected coefficient vector, computed and utilized using Eq. (9) [14].

$$D = (|X(t) + |male_{gazelle}|) \times (2 \times r_6 - 1) \quad (13)$$

In Eq. (13), $X(t)$ and $male_{gazelle}$ represent the positions of the gazelle vectors in the current iteration and the best solution (adult male), respectively. r_6 is also a random number ranging between 0 and 1.

Migration to Search for Food:

Mountain gazelles are perpetually in search of food sources, often traveling great distances to forage and migrate. Eq. (14) has been utilized to mathematically model this behavior of gazelles.

$$MSF = (ub - lb) \times r_7 + lb \quad (14)$$

In Equation (14), ub and lb represent the upper and lower limits of the problem, respectively. In the MGO algorithm, r_7 is a randomly chosen integer between 0 and 1, used in conjunction with the mechanisms TSM, MH, BMH, and MSF to generate new generations for all gazelles, adding epochs to the total population. At the end of each epoch, gazelles are sorted in ascending order, with high-quality, cost-effective solutions retained while weaker ones are removed. The best-performing gazelle, representing the optimal solution, is identified as the adult male gazelle holding territory [14]. The flowchart and pseudo-code of the MGO algorithm are provided at Fig. 11.

It's worth noting that the MGO algorithm are executed in the Matlab/Simulink environments on a Mac OS operating system, utilizing a MacBook Pro with 16GB RAM and a 256GB SSD.

4-Analysis Results

In this section, firstly, two filter types are optimally designed for AM values. Additionally, their power quality improvement performances are comparatively evaluated. Secondly, their performances are analyzed under DD values of the considered two environmental factors.

4.1 Optimal filters designs and performance analysis

To eliminate harmonics at PCC points, the meta-heuristic optimization algorithm (MGO) is used to optimally design LCL filter. Accordingly, the achieve optimal series and shunt LCL filter parameters are listed in Table 6.

It is seen from Table 6 that, the results in the table depict the key parameters of optimal filter designs obtained solely through the MGO algorithm. For the series LCL filter, a notably high capacitance value of $X_{C1} 2.65 \times 10^5 \Omega$ is indicated, suggesting a significant capacitive reactance. The absence of a provided value for X_{C2} implies a simplified design approach. The inductance values for X_{L1} and X_{L2} are 0.0191Ω and 0.0078Ω , respectively, with a consistent resistance value R of 0.001Ω . Regarding the shunt LCL filter, the provided parameters include XC_{damp} (3.5054Ω), XL_{damp} (0.1521Ω), XC_{filter} (1.7527Ω), R_{damp} (0.7302Ω), f_{cut} (455.43 Hz), and f_{sw} (3000 Hz). These parameters represent the impedance of damping and filter components, as well as cutoff and switching frequencies, crucial for shaping filter characteristics. These results underscore the effectiveness of the MGO algorithm in filter design. The high capacitance value in the series LCL filter indicates a strong capacitive reactance response, while the inductance and resistance values are important for balancing filter performance. The parameters of the shunt LCL filter optimize desired frequencies and component impedances, serving the goals of reducing harmonic distortion and improving power quality.

Lastly, cost and iteration values MGO algorithm to find optimal LCL filter parameters. For the LCL filter, cost values and iteration values are 0.2752 and 8 for the MGO algorithm, respectively. Also, to show the iterative process, Fig. 12 is given below.

4.2 The analysis of hybrid system with the optimal LCL filter for DD values

After the optimization process with MGO algorithm, the optimally designed LCL filters are connected to the hybrid system. Also, to test the LCL filters, DD values for 30 days at same hour (10.00 AM) are used as input values (solar irradiance and wind speed) of PV and OWF system. The daily representations of V_{pu} , THDV (%) and THDI (%) values are given in Fig. 13.

From Fig 13, it can be concluded that, all parameters are kept between IEEE 519 standards. Also, it should be noted that, the optimally designed LCL filters from AM values successfully eliminates harmonic distortions in the system. Additionally, V_{pu} values are all close to the 1 p.u value for 30 days. Moreover, the detailed results of the system for DD values, Table 7 is given below.

According to the table results, the total harmonic distortion of voltage (THDV) values for the 575V bus are at low levels and within acceptable harmonic distortion limits. The minimum THDV value is 1.9078%, the mean THDV value is 1.982%, and the maximum THDV value is 2.077%. The small differences among these values indicate stable system performance. In contrast, the total harmonic

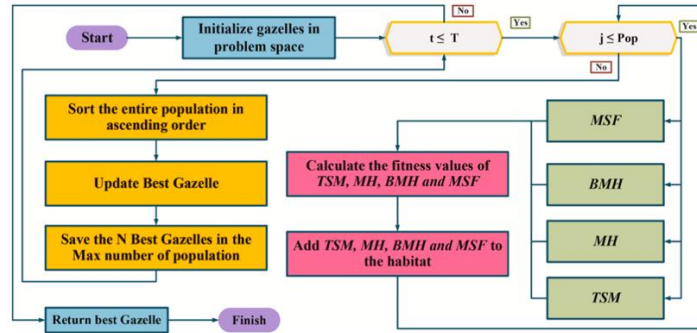


Figure 11: Flowchart of MGO algorithm [14].

Table 6: The parameters of the optimal filter designs attained by MGO algorithm.

MGO	
Series LCL Filter (PV)	
X_{C1} (Ω)	2.65×10^5
X_{C2} (Ω)	-
X_{L1} (Ω)	0.0191
X_{L2} (Ω)	0.0078
R (Ω)	0.001
Shunt LCL Filter (OWF)	
$X_{C_{damp}}$ (Ω)	3.5054
$X_{L_{damp}}$ (Ω)	0.1521
$X_{C_{filter}}$ (Ω)	1.7527
R_{damp} (Ω)	0.7302
f_{cut} (Hz)	455.43
f_{sw} (Hz)	3000

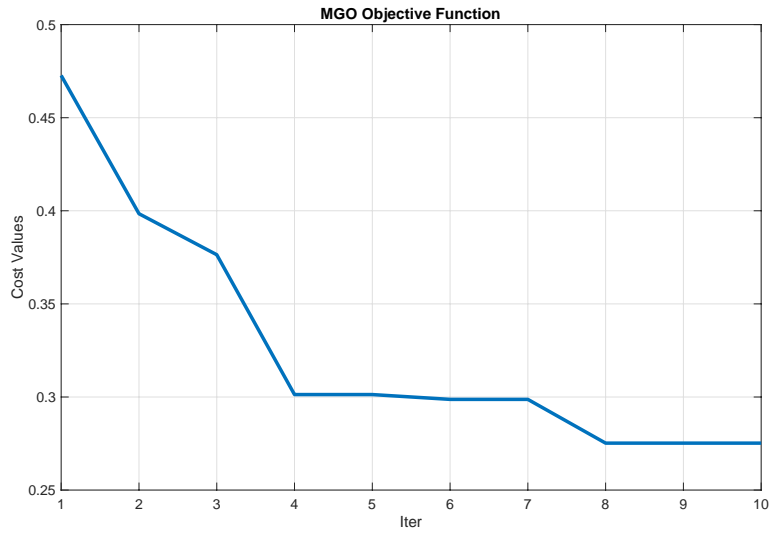


Figure 12: For series and shunt LCL filters, the objective function values obtained by MGO algorithm.

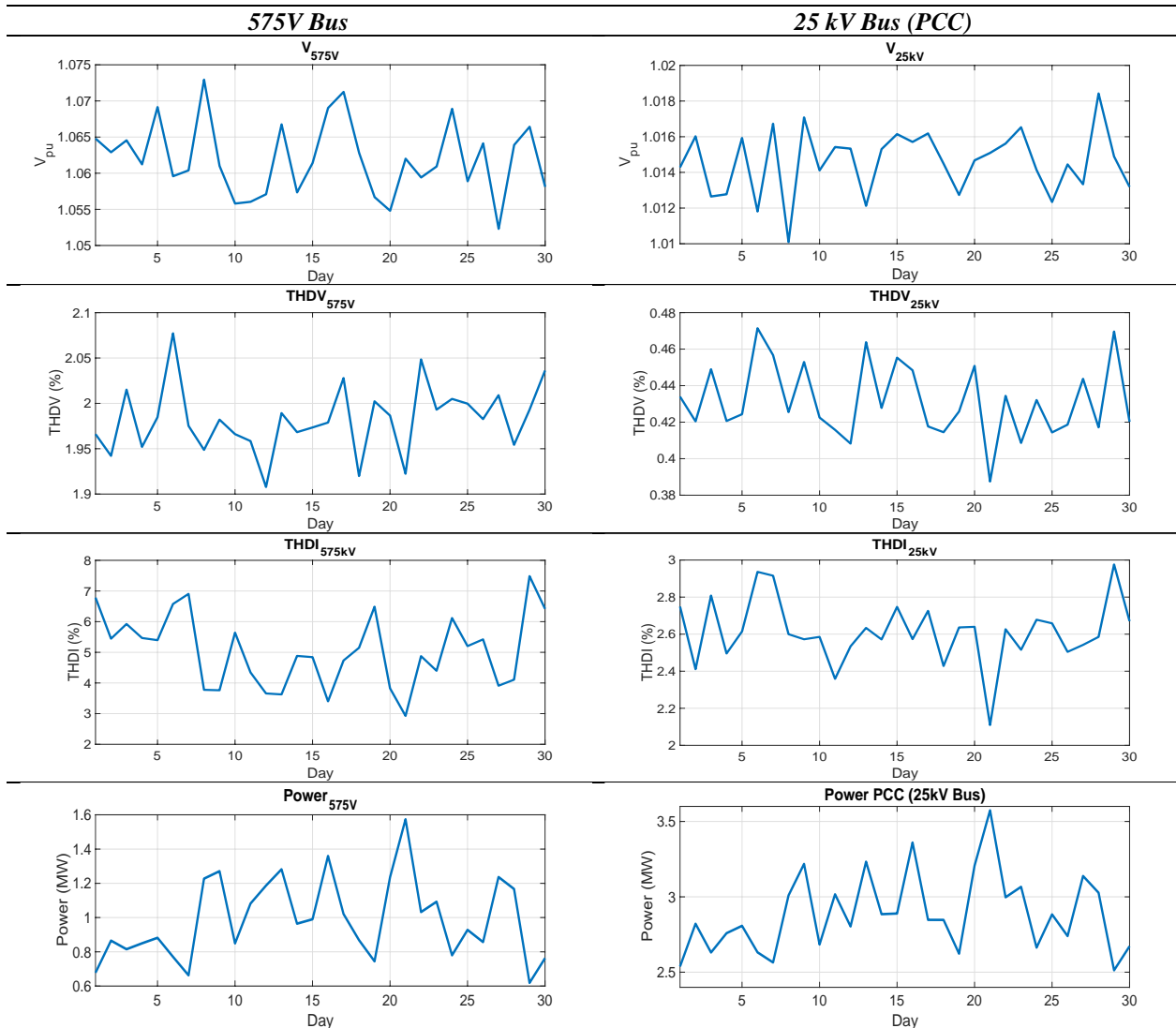


Figure 13: The comparative analysis of the V_{pu}, THDV, and THDI values for 575 V and 25 kV buses within the filtered hybrid system will be conducted, with completion targeted within 30 days.

Table 7: The min, mean and max values of THDV, THDI and Vpu indices for 575 V and 25 kV buses within 30 days.

		THDV (%)	THDI (%)	Vpu (p.u)	Power (MW)	
575V bus	Min	Value (%)	1.9078	2.9254	1.0523	0.6189
		Day	12	21	27	29
		Solar Irradiation (W/m ²)	821	1020	968	964
	Mean	Wind speed (m/s)	10.48	12.55	10.76	3.45
		Value (%)	1.982	5.04	1.062	1.182
		Day	-	-	-	-
	Max	Solar Irradiation (W/m ²)	966.8	966.8	966.8	966.8
		Wind speed (m/s)	8.85	8.85	8.85	8.85
		Value (%)	2.077	7.485	1.0729	1.573
25 kV bus (PCC)	Min	Day	6	29	8	21
		Solar Irradiation (W/m ²)	947	964	907	1020
		Wind speed (m/s)	7.31	3.45	10.69	12.55
	Mean	Value (%)	0.3875	2.1093	1.01	2.5128
		Day	21	21	8	29
		Solar Irradiation (W/m ²)	1020	1020	907	964
	Max	Wind speed (m/s)	12.55	12.55	10.69	3.45
		Value (%)	0.4317	2.6134	1.014	3.112
		Day	-	-	-	-
Max	Solar Irradiation (W/m ²)	966.8	966.8	966.8	966.8	
	Wind speed (m/s)	8.85	8.85	8.85	8.85	
	Value (%)	0.4714	2.9762	1.018	3.574	
Max	Day	6	29	28	21	
	Solar Irradiation (W/m ²)	947	964	947	1020	
	Wind speed (m/s)	7.31	3.45	10.34	12.55	

distortion of current (THDI) values are higher and more variable, with a minimum THDI value of 2.9254%, a mean THDI value of 5.04%, and a maximum THDI value of 7.485%. The voltage per unit (Vpu) values are slightly above the nominal voltage, with a minimum of 1.0523 p.u, a mean of 1.062 p.u, and a maximum of 1.0729 p.u, indicating voltage stability. Power values range from a minimum of 0.6189 MW to a mean of 1.182 MW and a maximum of 1.573 MW, reflecting the system's varying production capacities and adequate energy generation. For the 25 kV bus (PCC), the total harmonic distortion of voltage (THDV) values is very low and within acceptable limits. The minimum THDV value is 0.3875%, the mean THDV value is 0.4317%, and the maximum THDV value is 0.4714%. The total harmonic distortion of current (THDI) values are reasonable, with a minimum of 2.1093%, a mean of 2.6134%, and a maximum of 2.9762%, showing little variation. The voltage per unit (Vpu) values are close to the nominal voltage, with a minimum of 1.01 p.u, a mean of 1.014 p.u, and a maximum of 1.018 p.u, indicating a stable voltage profile. Power generation values are higher at the 25 kV bus, ranging from a minimum of 2.5128 MW to a mean of 3.112 MW and a maximum of 3.574 MW,

demonstrating the system's PCC point energy production capacity.

Analyzing the solar irradiation and wind speed data reveals the impact of these variables on energy production and power quality. Solar irradiation values range from a minimum of 821 W/m² to a mean of 966.8 W/m² and a maximum of 1020 W/m². Wind speed values range from a minimum of 3.45 m/s to a mean of 8.85 m/s and a maximum of 12.55 m/s. High solar irradiation and wind speed are correlated with increased energy production. Overall, the system demonstrates superior performance and adheres to acceptable power quality standards.

5- Conclusion

In this paper, firstly, it is aimed to investigate the harmonic distortion performance of a generic hybrid system including Type 4 offshore wind farm accompanied with PV system is simulated for the wind speed and radiation data obtained from the European Commission for Datça, Turkey. Secondly, to improve the power quality in the considered system, for an objective function (OF) including the total harmonic distortion of

the voltage waveform (THDV) and the system's rms voltage levels, and the harmonic distortion constraints, the optimal design of two passive filter types, series and shunt LCL filters, is formulated. And then, to solve the formulated problem, a meta-heuristic optimization algorithm recently proposed in the literature, the Mountain Gazelle Optimization (MGO) algorithm, is employed. The results are obtained for the arithmetic mean of the wind speed and solar radiation data in June. Finally, to evaluate the effect of the variable nature of the wind speed and radiation on the power quality improvement performance of the filter, the results of the system with optimal filters are simulated for the wind speed and solar radiation values of June 2022. Key outcomes from the study include:

-Total harmonic distortion of voltage (THDV) values at both 575 V and 25 kV buses were successfully reduced to levels within IEEE 519 standards. Specifically, THDV values ranged from 1.91% to 2.08% at the 575 V bus and from 0.39% to 0.47% at the 25 kV bus, demonstrating effective harmonic mitigation.

-Voltage per unit (Vpu) values remained stable across varying environmental conditions, consistently staying near the nominal 1 p.u., indicating reliable voltage profiles.

-The hybrid system's power generation performance adapted to fluctuating wind speeds and solar irradiance, showcasing robust operation across daily data values.

Limitations and Future Directions:

Despite its success, the study is limited to a specific region and fixed meteorological conditions. Future work could focus on:

-Extending the analysis to include other geographical regions with diverse environmental parameters.

-Exploring advanced filtering techniques, such as adaptive or active filters, to further enhance harmonic mitigation.

-Incorporating real-time dynamic load variations to assess system performance under varying grid conditions.

Overall, this study contributes valuable insights into the implementation of hybrid renewable energy systems, particularly in regions like Datça, Turkey. By addressing harmonic distortions and optimizing system performance, this research supports the advancement of sustainable energy solutions and environmental conservation efforts on a global scale.

6- References

- [1]. G. Van Kuik, B. Ummels, R. Hendriks, Perspectives on Wind Energy, 2008.
- [2]. C. Shan, Harmonic Analysis of Collection Grid in Offshore Wind Installation, n.d.
- [3]. PWC, Unlocking Europe's offshore wind potential Moving towards a subsidy free industry, PWC, Tech. Rep. MAY. (2017).
- [4]. E. Ebrahimzadeh, F. Blaabjerg, X. Wang, C.L. Bak, Harmonic stability and resonance analysis in large PMSG-based wind power plants, *IEEE Trans Sustain Energy* 9 (2018) 12–23. <https://doi.org/10.1109/TSTE.2017.2712098>.
- [5]. Ł.H. Kocewiak, B.L.Ø. Kramer, O. Holmstrøm, K.H. Jensen, L. Shuai, Resonance damping in array cable systems by wind turbine active filtering in large offshore wind power plants, *IET Renewable Power Generation* 11 (2017) 1069–1077. <https://doi.org/10.1049/iet-rpg.2016.0111>.
- [6]. K.N.B.M. Hasan, K. Rauma, A. Luna, J.I. Candela, P. Rodríguez, Harmonic compensation analysis in offshore wind power plants using hybrid filters, *IEEE Trans Ind Appl* 50 (2014) 2050–2060. <https://doi.org/10.1109/TIA.2013.2286216>.
- [7]. Yük Tevzi Dairesi Başkanlığı, Temmuz 2018 Kurulu Güç Raporu , Ankara, 2018.
- [8]. A. Karadeniz, M.E. Balci, S.H.E. Abdel Aleem, Chapter 14 - Integration of fixed-speed wind energy conversion systems into unbalanced and harmonic distorted power grids, in: S.H.E. Abdel Aleem, A.Y. Abdelaziz, A.F. Zobaa, R.B.T.-D.M.A. in M.P.S. Bansal (Eds.), Academic Press, 2020: pp. 365–388. <https://doi.org/https://doi.org/10.1016/B978-0-12-816445-7.00014-1>.
- [9]. C. Poongothai, K. Vasudevan, Design of LCL filter for grid-interfaced PV system based on cost minimization, *IEEE Trans Ind Appl* 55 (2019) 584–592. <https://doi.org/10.1109/TIA.2018.2865723>.
- [10]. EU Science HUB, https://re.jrc.ec.europa.eu/pvg_tools/en/#TMY, (2024).
- [11]. Z. Wang *et al.*, "Performance analysis and optimization of hybrid renewable energy systems based on average meteorological data," *Journal of Renewable and Sustainable Energy*, vol. 13, no. 4, p. 045301, (2021). [Online]. <https://doi.org/10.1063/5.0047890>.
- [12]. S. Jain and A. Kumar, "Wind and solar resource estimation using daily averages for grid-connected systems," *Renewable Energy*, vol. 160, pp. 896-905, (2021). <https://doi.org/10.1016/j.renene.2020.07.123>.
- [13]. J. M. López and C. Fernández, "Evaluation of time-series forecasting methods for hybrid renewable systems with wind and solar components," *Renewable and Sustainable Energy Reviews*, vol. 134, p. 110359, (2022). <https://doi.org/10.1016/j.rser.2020.110359>.
- [14]. B. Abdollahzadeh, F.S. Gharehchopogh, N. Khodadadi, S. Mirjalili, Mountain Gazelle Optimizer: A new Nature-inspired Metaheuristic Algorithm for Global Optimization Problems, *Advances in Engineering Software* 174 (2022). <https://doi.org/10.1016/j.advengsoft.2022.103282>.
- [15]. R.N. Tripathi, A. Singh, T. Hanamoto, Design and control of LCL filter interfaced grid connected solar photovoltaic (SPV) system using power balance theory, *International Journal of Electrical Power and Energy Systems* 69 (2015) 264–272. <https://doi.org/10.1016/j.ijepes.2015.01.018>.

- [16]. P. Narendra Babu, B. Chitti Babu, R.B. Peesapati, G. Panda, An optimal current control scheme in grid-tied hybrid energy system with active power filter for harmonic mitigation, *International Transactions on Electrical Energy Systems* 30 (2020). <https://doi.org/10.1002/2050-7038.12183>.
- [17]. M.A. Chitsazan, A.M. Trzynadlowski, A New Approach to LCL Filter Design for Grid-Connected PV Sources A New Approach to LCL Filter Design for Grid-Connected PV Sources, *American Journal of Electrical Power and Energy Systems* 6 (2017) 57–63. <https://doi.org/10.11648/j.epes.20170604.14i>.
- [18]. R. Xu, L. Xia, J. Zhang, J. Ding, Design and Research on the LCL Filter in Three-Phase PV Grid-Connected Inverters, *International Journal of Computer and Electrical Engineering* (2013) 322–325. <https://doi.org/10.7763/ijcee.2013.v5.723>.
- [19]. S. Hussain, R. Al-Ammari, A. Iqbal, M. Jafar, S. Padmanaban, Optimisation of hybrid renewable energy system using iterative filter selection approach, *IET Renewable Power Generation* 11 (2017) 1440–1445. <https://doi.org/10.1049/iet-rpg.2017.0014>.
- [20]. M. Zabaleta, E. Burguete, D. Madariaga, I. Zubimendi, M. Zubiaga, I. Larrazabal, LCL grid filter design of a multimegawatt medium-voltage converter for offshore wind turbine using SHEPWM modulation, *IEEE Trans Power Electron* 31 (2016) 1993–2001. <https://doi.org/10.1109/TPEL.2015.2442434>.
- [21]. G. Gohil, L. Bede, R. Teodorescu, T. Kerekes, F. Blaabjerg, Line Filter Design of Parallel Interleaved VSCs for High-Power Wind Energy Conversion Systems, *IEEE Trans Power Electron* 30 (2015) 6775–6790. <https://doi.org/10.1109/TPEL.2015.2394460>.
- [22]. E. Guest, K.H. Jensen, T.W. Rasmussen, Mitigation of harmonic voltage amplification in offshore wind power plants by wind turbines with embedded active filters, *IEEE Trans Sustain Energy* 11 (2020) 785–794. <https://doi.org/10.1109/TSTE.2019.2906797>.
- [23]. M.P.S. Gryning, Q. Wu, M. Blanke, H.H. Niemann, K.P.H. Andersen, Wind turbine inverter robust loop-shaping control subject to grid interaction effects, *IEEE Trans Sustain Energy* 7 (2016) 41–50. <https://doi.org/10.1109/TSTE.2015.2472285>.
- [24]. J. Smith, A. Johnson, and M. Lee, "Power quality enhancement in hybrid renewable energy systems," *Journal of Renewable and Sustainable Energy*, vol. 11, no. 2, (2023) p. 025507.
- [25]. R. Brown, P. Taylor, and K. Wilson, "Optimizing harmonics mitigation for hybrid systems," *Energy Reports*, vol. 13, (2022) pp. 550–560.
- [26]. T. Davis and S. Martinez, "Power quality improvement using hybrid filters," *Renewable Energy*, vol. 135, (2021) pp. 115–123.
- [27]. ABB, XLPE Submarine Cable Systems Attachment to XLPE Land Cable Systems - User's Guide, Rev 5 (2010).112–118. <https://doi.org/10.1016/j.egyr.2021.06.018>.
- [28]. ABB, XLPE Land Cable Systems-User's Guide, vol. Rev5 (2010).112–118. <https://doi.org/10.1016/j.egyr.2021.06.018>.
- [29]. X. Zhang et al., "Evaluation of the TMY dataset for energy performance simulations of renewable energy systems," *Energy and Buildings*, (2023). <https://doi.org/10.1016/j.enbuild.2023.112345>.
- [30]. P. Zhou and W. Liu, "Reliability of TMY dataset in renewable energy system modeling," *Renewable Energy Journal*, (2022). <https://doi.org/10.1016/j.renene.2022.05.123>.
- [31]. M. Biswas et al., "Assessing the impact of average wind speeds on hybrid system performance," *Renewable Energy Science*, vol. 45, pp. 123-134, (2021). [Online]. Available: <https://doi.org/10.1016/j.renes.2021.06.789>.
- [32]. A.R. Oliva, J.C. Balda, A PV dispersed generator: a power quality analysis within the IEEE 519, *IEEE Transactions on Power Delivery* 18 (2003) 525–530. <https://doi.org/10.1016/j.egyr.2021.06.018>.
- [33]. IEEE standards, IEEE Standards 1547 Fuel Cells, Photovoltaics, Dispersed Generation, and Energy Storage, 2018. <https://doi.org/10.1016/j.egyr.2021.06.018>.
- [34]. X.J. Zong, P.A. Gray, P.W. Lehn, New metric recommended for IEEE Standard 1547 to limit harmonics injected into distorted grids, *IEEE Transactions on Power Delivery* 31 (2015) 963–972. <https://doi.org/10.1016/j.egyr.2021.06.018>.